

A Revised Water Vapor Product for the SAGE II Version 6.2 Data Set

Larry W. Thomason

NASA Langley Research Center, Hampton, Virginia, USA

Sharon P. Burton and Nina Iyer

Science Applications International Corporation, Hampton, Virginia, USA

Joseph M. Zawodny

NASA Langley Research Center, Hampton, Virginia, USA

John Anderson

Hampton University, Hampton, Virginia, USA

Abstract. The SAGE II (Stratospheric Aerosol and Gas Experiment) water vapor retrieval process has been updated to reflect a new understanding of the instrument performance. Primarily this is reflected in a shifted spectral response for the primary water channel near 935 nm for the period after January 1986. In addition, the water vapor and ozone spectroscopy, aerosol clearing process, and error estimation have been updated. The end result is that the measurement bias observed in version 6.1 and earlier versions has been effectively eliminated. The sensitivity to aerosol has been reduced so that the recommended upper limit for usable water vapor is now $3 \cdot 10^{-4} \text{ km}^{-1}$ in 1020-nm aerosol extinction. The comparable value for Version 6.1 was $\sim 2 \cdot 10^{-5} \text{ km}^{-1}$ or 10 times more sensitive than in the new version. The impact of the channel drift on the retrieved water vapor relative to the simple model employed in this version will be difficult to separate from geophysical change and therefore caution is recommended in evaluating trends derived from this data set.

1. Introduction

The Stratospheric Aerosol and Gas Experiment II (SAGE II) has been operational since October 1984 aboard the Earth Radiation Budget Satellite and has now completed more than 19 years of operation. The instrument has seven channels nominally located at 386, 448, 452,

525, 600, 935, and 1020 nm and employs the solar occultation technique to measure multi-wavelength line-of-sight atmospheric transmission profiles during each sunrise and sunset encountered by the spacecraft. From the transmission profiles, vertical profiles of ozone, nitrogen dioxide, aerosol extinction at 386, 452, 525, and 1020 nm, and water vapor can be derived [Chu et al., 1989; Zawodny et al., 2000]. With its exceptional lifetime and stability, SAGE II has become a cornerstone in studies of stratospheric change particularly related to ozone and aerosol [e.g., Solomon et al., 1996; Thomason et al., 1997a; Thomason et al., 1997b; Cunnold et al., 2000; Wang et al., 2002; Newchurch et al., 2003] including playing a key role in numerous international assessments [e.g., SPARC, 1998]. SAGE II water vapor measurements have the potential for similar interest but have historically been considerably less useful due to well known deficiencies in the data in previous versions. For example, it has been well known that the retrieval is highly sensitive to even modest levels of aerosol extinction [Chu et al., 1993; Chiou et al., 1993]. In fact, it is not uncommon for the effects of molecular scatter, ozone absorption, as well as aerosol scattering to each be larger than water vapor absorption in the ostensible water vapor channel (935 nm). In the stratosphere, water vapor is typically between 5 and 10% and only rarely more than 15% of the total signal in this channel below 30 km. As a result, even under the most optimal conditions, the retrieval of water vapor from SAGE II measurements is challenging.

In recent years, SAGE II processing algorithms went through a series of major revisions leading to the release of Version 6.0 in June 2000 and Version 6.1 in October 2001. The last pre-version 6.0 version of water vapor, usually referenced as 5.9, was the subject of a special section in a 1993 issue of the *Journal of Geophysical Research* [see Chu et al., 1993 and following papers]. Version 5.9, which included only 1985 through 1990 in public release, was

not a robust version and exhibited anomalous behavior that included a significant drift in the water vapor mixing ratio around the hygropause and to a lesser extent at other altitudes [McCormick et al., 1993]. This version produced reasonable depictions of seasonal variations in the lower stratosphere at middle latitudes but did not produce well-known seasonal cycles in the tropics [SPARC, 2000] including the tropical tape recorder [Mote et al. 1996]. For Version 5.9 and earlier, water vapor maintained separate versioning and, in fact, some aspects of data processing were not well synchronized with the software that produced the other species. Only modest changes were made to the water vapor retrieval for Versions 6.0 and 6.1. The water vapor and ozone spectroscopy were updated and the aerosol clearing methodology was made consistent with that used for clearing aerosol from the ozone channel (600 nm). At the same time, it was found that the molecular scattering cross section for the water vapor channel was incorrect and was more appropriate to a channel location close to nominal design location (940 nm) than for the preflight measured bandpass centered at 935 nm. The most obvious effect was for the water vapor product to become significantly drier, particularly around the hygropause, producing a bias at the hygropause relative to other measurement systems that was larger than reported for Version 5.9 [e.g., Chiou et al. 1992, Rosenlof et al., 2001].

Since the release of Version 6.1, development work on the operational SAGE II algorithm has been focused on improving the water vapor retrieval algorithm and Version 6.2, released in October 2003, is primarily the outcome of that effort. Herein, we describe the process by which we identified an apparent change in the spectral response in the water vapor channel and estimated the new channel spectral response. Based on the new channel location, SAGE II Version 6.2 water vapor is evaluated and we demonstrate that Version 6.2 water vapor represents a significant step forward in the quality of this product.

2. Diagnosing the Water Vapor Retrieval Algorithm Problem

The Version 6.1 water vapor algorithm is not significantly different than the one described in Chu et al. [1993]. Essentially the line-of-sight (LOS) water vapor optical depth is extracted from the LOS optical depth in the 935-nm channel by

$$\tau_{H_2O} = \tau_{935} - \sigma_{air} n_{air} - \sigma_{o_3} n_{o_3} - \tau_{aerosol} \quad (1)$$

where σ_{air} and σ_{O_3} are the cross sections of air and ozone at 935 nm, n_{air} is the LOS air number density computed from co-located NCEP profiles, n_{O_3} is the LOS ozone number density computed using the other 6 SAGE II channels, and $\tau_{aerosol}$ is the estimated LOS aerosol optical depth at 935 nm.

Following Chu et al. [1993], the water vapor mixing ratio is retrieved from the optical depth residual, τ_{H_2O} , using a straight-forward onion-peel, iterative Newton-Raphson approach in which the mixing ratio, χ , is solved for iteratively using

$$\chi_n = \chi_{n-1} + \left(\frac{dA}{d\chi} \right)^{-1} \Delta A_n, \quad (2)$$

where A is water vapor absorption (or $1 - \exp(-\tau_{H_2O})$), $dA/d\chi$ is the derivative of absorption to a unit change in mixing ratio, and n is the iteration step number. The Emissivity Curve-of-Growth Approximation is used for the forward model (the mixing ratio to absorption calculation) and computing the derivative term. Apart from the channel location problem, the water vapor measurement is robust and, for a wide variety of inversion techniques, there is little difference in the inverted product. For historical and continuity reasons, the existing inversion method has been used in Version 6.2. SAGE II LOS optical depth profiles are calculated at a 0.5-km resolution and most products are reported at this resolution. However, to reduce noise, the vertical

profiles of water vapor absorption are smoothed to approximately 1-km resolution below 25 km using 1-2-1 smoothing and to approximately 2.5-km resolution above 30 km using 1-1-1-1 smoothing with a transition between 25 and 30 km.

In Version 5.9, estimation of the aerosol contribution at 935 nm was based on a simple one-parameter aerosol size distribution that relied on the 525 to 1020-nm LOS aerosol optical depth ratio [Thomason, 1991]. In Version 6.0 and following versions, the standard model is based on a fit of 935-nm to 1020-nm aerosol optical depth ratio with the 525 to 1020-nm aerosol optical depth ratio where both ratios are computed using Mie scattering and a family of log-normal size distributions with effective radii from 0.12 to 0.65 μm . The scatter around the fit is close to 1% for the expected range in the 525 to 1020-nm aerosol optical depth ratio and this residual uncertainty is included in the water vapor uncertainty budget. A number of prospective empirical and physically-based methods were evaluated for the estimation 935-nm aerosol optical depth [e.g., Steele et al., 1997]. However, SAGE II's aerosol clearing at 935 nm is effectively based on measurements at 525 and 1020 nm since the other SAGE II aerosol channels are even further away from 935 nm and carry little weight. The strategy of interpolating over a factor of two in wavelength is inadequate given the episodically enhanced aerosol loading during the SAGE II lifetime and the small magnitude of the water vapor signal. As a result, many models have been considered for this task and fail to varying degrees and in varying ways at high aerosol loading. The current model was selected based on its simplicity and its overall positive performance.

To understand the deficiencies in the existing water vapor data set, Version 6.1 water vapor was evaluated against a water vapor climatology derived from the Halogen Occultation Experiment (HALOE). The HALOE water vapor climatology (HC) is derived from HALOE

Version 19 H₂O data between January 1992 and December 2002. The climatology is a product of a regression of the long-term HALOE record with terms that included annual, semi-annual, and quasi-biennial cycles and a long-term linear trend. For the purposes of the evaluation, we excluded the linear trend term. For this experiment, HC is reported on an altitude grid between 15-50 km range and in 4° latitude increments from 58°S to 58°N. Data contaminated by the presence of cloud were identified and eliminated using the method of Hervig and McHugh [1999]. The HALOE climatology is convenient to use since it can be applied to the entire SAGE II lifetime, has a similar spatial coverage to SAGE II, and has been thoroughly evaluated in the refereed press [SPARC, 2000].

2.1 Aerosol Clearing Errors

Figure 1 shows a comparison of SAGE II version 6.1 water with the HALOE climatology for several altitude/latitude bands. The SAGE II-HC differences show discrepancies that are characteristic of the entire data set. First, there is an obvious sensitivity to enhanced aerosol particularly associated with Mt. Pinatubo (mid-1991 to at least the end of 1993) and to lesser degrees the aerosol enhancement at the start of the record (from the eruption of El Chichon in 1982) and in 1990 due to the eruption of Kelut. Figure 2 shows the stratospheric optical depth (the integrated column from the tropopause upward) in northern mid-latitudes for the period 1984 through 2000. The large enhancement associated with Pinatubo is clearly correlated to an excursion in the water vapor data shown in Figure 1 at least through the end of 1994. The Kelut eruption of February 1994 is a small aerosol event that nonetheless has a significant impact on the water vapor retrieval particularly in the lower tropical stratosphere. Significantly, though the problem with the SAGE II water vapor data is commonly attributed to aerosol interference [e.g., SPARC 2000], Figures 1 and 2 clearly show that the SAGE II dry

bias in the lower stratosphere, relative to HC, is remarkably constant even during periods when the aerosol levels continue to decline. For instance, the water vapor cycle at 42°N is fairly constant from early 1994 onwards even while the aerosol column level drops by more than a factor of five (and at some altitudes by more than a factor of 10) during this period. This pair of figures strongly argues that the dry bias cannot primarily be the result of poor aerosol clearing. The difference between the mean 1996-1999 Version 6.1 water vapor and HC is summarized in Figure 3 for northern mid-latitudes. The differences between 15 and 20 km are about 1.5 ppm, or almost a factor of two low, but decreases to zero around 28 km, and Version 6.1 is about 0.5 ppm wetter than HC above 30 km. Revisions in the processing for Version 6.2 water are focused on rectifying these low-aerosol loading discrepancies.

A different way to look at the water vapor problem is to reformulate Equation 1 so that the unknown is the 935-nm aerosol optical depth and to solve for it using HC to compute the expected water contribution, $\tau_{H_2O}^{HC}$, and removing the other terms as in the standard retrieval.

This can be expressed as

$$\tau_{aerosol} = \tau_{935} - \sigma_{air} n_{air} - \sigma_{o_3} n_{o_3} - \tau_{H_2O}^{HC}. \quad (3)$$

The computed aerosol can then be compared with the Version 6.2 aerosol model used in the standard retrieval. The results for this experiment are shown in Figure 4 for January data in 1985, 1986, 1996, and 1999. Interestingly, the agreement between the aerosol model and the HC-based estimates for the aerosol in January 1985 is fairly good and is within 1% over the observed range of 525 to 1020-nm optical depth ratio. However by 1986, this relationship is in considerably less harmony and the agreement is even worse by 1996 and 1999; years in which aerosol levels are considerably lower. Detailed examination of the results of this experiment demonstrates that assuming these relationships are correct would require an aerosol model that

is strongly time dependent and that would also need to exhibit strong latitudinal dependencies. An aerosol model based on these data requires a complexity incompatible with the success achieved with the same model strategy used in the aerosol clearing in Version 6.1 ozone [Wang et al., 2002] nor is it compatible with the relatively simple aerosol extinction spectra observed by SAGE III [Thomason and Taha, 2003]. Ultimately, it is apparent that the aerosol model is unlikely to be the primary cause for the observed dry bias.

2.2 Ozone Cross Section Error

Also requiring consideration as a possible source of the problem is the ozone cross section used in the retrieval [Shettle and Anderson, 1994]. For room temperature, the estimated uncertainty around 950 nm is estimated to be ~10% [Anderson and Mausberger, 1992; Anderson et al., 1993; SAGE III ATBD: Solar and Lunar Algorithms, 2002] but could be larger at stratospheric temperatures. Figure 5 shows the sensitivity of the retrieved water vapor to the ozone cross section. Even decreasing the cross section to zero changes the lower stratospheric water vapor by only about 1 ppm (about half of the target change) while generating catastrophic changes in the water vapor profile between 25 and 35 km. Therefore, changes to the ozone cross section alone are not sufficient to affect the desired changes to the water vapor profile.

2.3 Channel Location Drift

The final possible culprit for creating the observed SAGE II water vapor dry bias is a change in the spectral response of the water vapor channel. Changes in the spectral response would alter the contribution by molecular and aerosol scattering and ozone absorption as well as the strength of the water vapor absorption itself. Most SAGE II channels are defined by their position along a Rowland circle within the spectrometer and are therefore extremely stable in spectral response. However, interference filters are used in the spectrometer for the NO₂

channels at 448 and 452 nm and for the water vapor channel. It has been noted for some time that the channel at 448 nm had apparently significantly drifted from its original location and created a concomitant drift in the NO₂ product. As shown in Figure 6, this drift is obvious from the long-term changes in the measured extraterrestrial sensitivity of that channel. Most SAGE II channels show the expected slow decrease in the overall efficiency of the optical system but channel 6 (448 nm), increases rapidly over the first 2000 days of the SAGE II mission strongly suggesting that the filter had ‘opened up’ or become spectral broader in time. This has been modeled in the data processing since Version 5.96.

The water channel is located in the spectrometer zero-order and, like the NO₂ channels, its spectral characteristics are defined by an interference filter; in this case centered at 935 nm with a FWHM of 30 nm. Normally, we would expect adjacent channels like 935 nm and 1020 nm to follow a similar degradation in sensitivity with time much like that exhibited by the 525 and 600 nm channels. Interestingly, the 935-nm channel decreases much faster in the first year or so of operation than the nearby 1020-nm channel. The change in brightness relative to 1020 nm could be consistent with a shift toward longer wavelengths. After more than 20 years, none of the original filter material is available and the filter was manufactured by an undisclosed proprietary process by a company that is no longer in business. As a result, it is unfortunately not possible to test a similar filter in a laboratory to identify processes by which such a shift could occur.

A change in the filter characteristics would probably comprise both a wavelength shift and a broadening (or, less likely, a narrowing) of the range in the filter bandpass. These two factors have a non-linear effect on the water vapor retrieval due to the complex interactions of water vapor absorption and the removal of other species: ozone, aerosol, and molecular scatter. An

experiment to map the sensitivity of the derived water vapor mixing ratio profile to changes in the central wavelength and width of the filter response was carried out using MODTRAN (v4.7). In the experiment, the 'U.S. Standard Atmosphere, 1976' atmospheric model was used with the background stratospheric aerosol model scaled by a factor of 0.5 to more closely match clean periods observed in the SAGE II data set. The goal was to find a shift and width change that produced the SAGE II-HC differences shown in Figure 3 and thus infer a more representative channel location.

The impact of changes in the two parameters was modeled by comparing retrievals based on two different optical depth profiles ($\tau_{\text{H}_2\text{O}}$). The first profile is computed for the nominal channel location and width using MODTRAN. The second profile mimics a "broken" transmission profile by computing transmission using MODTRAN at a different channel location and width but clearing the effects of ozone, aerosol, and molecular scattering based on the nominal channel response. The transmission profiles undergo vertical inversion to water vapor mixing ratio using the usual SAGE II process with water vapor spectroscopy for the nominal channel location.

Figures 7a and 7b show the effect of changing central wavelength and width of the filter location while holding the other parameter constant. Increasing the central wavelength has the generally positive feature of producing a maximum difference near 16 km (of the correct sign). At the same time, however, as the magnitude of the water vapor approaches the desired change of -1.5 ppm around 16 km, the change above 25 km becomes larger than desired +0.5 ppm. In contrast, changing just the width has a nearly constant effect over almost the entire altitude range shown, except below the hygropause. Based on these two figures, it appeared that a 5 nm shift combined with a change in the width would provide a good match for observed SAGE

II-HC bias. However, the two parameters interact in a non-linear fashion, and the apparent lack of altitude dependence for a shift in the width does not hold well at shifted wavelengths and no good match was found at a 5 nm shift (Figure 7c). Through a process of trial and error, the best match was found at a wavelength shift of 10 nm, with the filter width broadened by 10%. This curve is shown in Figure 7d. The maximum change is of approximately the right value, 1.5 ppm, though it is at a lower altitude than the maximum altitude (19 km) shown in Figure 3. The crossover from dryer to wetter occurs at 25 km and is a little lower than the target profile in Figure 3.

A test with the revised location was run with SAGE II processing code with the database recalculated at a shift of 10 nm and 10% broadening. Figure 8 shows the effect on 18 events in the latitude band 40°-44° N in June 1999. This figure shows reasonable agreement with the MODTRAN-based experiment and target difference profile in Figure 3 above the hygropause. As the result of the experiment, a modified filter bandpass was adopted (center 945 nm, 33 nm FWHM) and was subsequently introduced into the SAGE II processing and clearing of aerosol, ozone, and molecular effects based on the new location. Figure 9 shows the mean difference between SAGE II and HC for the new version 6.2 water vapor product for mid-latitudes between 1996 and 1999 (the Version 6.2 equivalent of Figure 3) that shows on average, the difference between HC and SAGE II Version 6.2 in this period is close to zero from 15 to 28 km and is about 0.4 ppm above 30 km. The agreement demonstrates that the goal of eliminating the differences shown in Figure 3 has been obtained to a great extent.

Operationally, since the channel location apparently shifted rapidly through 1985, Version 6.2 uses the original water vapor channel location through the end of 1985 and the new channel location beginning in 1986 with no accommodation for a gradual shift in wavelength. As a

result, water vapor data in 1985 should be used cautiously. Over longer time scales, changes to the water distribution, (i.e., trends) are likely to reflect the robustness of the revised channel location as well as geophysical changes to the water distribution. For instance, a 1-nm drift to longer wavelengths between 1986 and 2002 would produce about a -0.07 ppm/year change fairly consistently at and above the hygropause. Similarly, a 10% increase in width over the 16-year period change yields about a -0.015 ppm/year change at and above the hygropause. Efforts to derive geophysical trends from this data set must account for this effect.

Figure 10 shows the water vapor time series from SAGE II version 6.2, with HC overlaid again as in Figure 1. The agreement in magnitude and seasonal cycle is substantially improved. It is important to note that the channel locations parameters were derived to match a mean comparison between SAGE II version 6.1 and the HALOE climatology at a single latitude, averaged over 4 years and has no altitude, seasonal, or temporal component. That SAGE II water vapor now agrees well with HALOE over a large range of altitudes and latitudes and over a large range of aerosol levels strongly argues that the new location is correct. Detailed validation of the Version 6.2 water vapor product against other satellite-based measurements can be found in Taha et al. [2004] and against shuttle-based and balloon-borne systems in Chiou et al. [2004]. The comparisons shown in these papers further demonstrate the quality of the new version.

3. Sources of Error

The water vapor mixing ratio uncertainty, σ_{χ} , reported in the data product is total absorption uncertainty, σ_A , computed as the root mean-squared of the transmission uncertainty combined with the uncertainty in the removal of air density, ozone, and aerosol. The mixing ratio uncertainty is computed as

$$\sigma_{\chi}^2 = \sigma_A^2 \left(\frac{dA}{d\chi} \right)^{-2}. \quad (4)$$

The retrieval process amplifies relative transmission errors because unpeeling from the line-of-sight geometry to a vertical magnifies errors even in better behaved species like ozone and aerosol. In addition, since the water vapor absorption band ($\rho\sigma\tau$) follows strong-band absorption characteristics, errors in the LOS water vapor optical depth are approximately doubled in their impact on the retrieved water vapor profile. Figure 11 shows the mean propagation of uncertainty in the water vapor absorption into the retrieved mixing ratio for mid-latitude events in June 2002. The error magnification, which includes strong line and LOS-to-profile effects, is about a factor of seven for this period.

Figure 12 shows the fractions of the water vapor channel's total optical depth that comes from water vapor absorption. It is not uncommon, particularly just above the tropopause, for that fraction to be significantly less than 5%. Following Pinatubo, the fraction of signal from water vapor is less than 5% below 30 km and is often less than 1%. That the water vapor signal is such a small fraction of the total channel signal puts an enormous burden on the estimation of the aerosol contribution. In practice, the amplification of aerosol uncertainty into the water vapor mixing ratio uncertainty is about a factor of 7 during the lowest aerosol loading periods (2002) and close to 300 immediately after the Pinatubo eruption. As a result, even after correcting the location of the water vapor channel, the largest source of residual bias is associated with the removal of aerosol. As shown in Figures 1 and 9, non-physical, aerosol-driven bias has been significantly ameliorated for volcanically enhanced periods. The mean difference between SAGE II water vapor and HC as a function of 1020-nm aerosol extinction are shown in Figure 13 for Versions 6.1 and 6.2. For enhanced aerosol, Version 6.2 shows a

>5% departure when 1020-nm aerosol extinction is greater than $3 \cdot 10^{-4} \text{ km}^{-1}$. The comparable value for Version 6.1 is $\sim 2 \cdot 10^{-5} \text{ km}^{-1}$ (though for an oppositely signed departure) or more than a factor of 10 more sensitive than in the new version. The differences at low aerosol extinction are an altitude effect (shown in Figure 9) rather than sensitivity to aerosol. Given the rapidity with which the water vapor artifacts increase as 1020-nm aerosol extinction increases beyond $3 \cdot 10^{-4} \text{ km}^{-1}$, excluding water vapor measurements made for higher extinctions is recommended. This limit excludes data primarily in the periods immediately after launch from 1984 through 1986 and after the Pinatubo eruption through 1994 and has only a minor impact in the rest of the record. For individual profiles and/or locations, the limiting aerosol extinction value may be different. Given the burden made on the aerosol model and that so much of the data now seems useable indicates that the aerosol model is functioning extremely well.

Nominally, the influence of ozone on the water vapor retrieval is minimal. SAGE II LOS ozone uncertainty is on the order of 1% and is only a small part of the overall uncertainty budget. Since there is some uncertainty in the ozone cross section, however, the possibility of some bias in the water vapor product exists. Since the channel location process was predicated in part on ozone spectroscopy, a significant modification to the ozone cross section might suggest the need to repeat the channel location sensitivity study described in this paper.

4. Conclusions

SAGE II Version 6.2 water is built upon the realization that the filter used to define the spectral characteristics of the water vapor channel had drifted significantly from its pre-launch location. Through a sensitivity study based on a multi-year departure from the HALOE water climatology and MODTRAN, a revised location and width 10 nm toward longer wavelengths and 10% width increase was inferred. The shift in location is larger than comfortable but the performance of the

resultant product argues that the location is very close to the mark. With the new location, the dry bias with respect to HALOE has been effectively eliminated and the sensitivity to aerosol clearing substantially reduced. One hallmark of the new version is that the tropical tape recorder, among other features, previously nearly undetectable, can now be clearly seen (Figure 14) in the data set. However, in Version 6.2, significant sensitivity to aerosol remains and the water vapor product should not be used when 1020-nm aerosol extinction is greater than $3 \cdot 10^{-4} \text{ km}^{-1}$. Given a 19-year record, an assessment of trends in stratospheric water vapor over this period would be a desirable by-product of the algorithm revision [e.g., Rosenlof et al., 2001]. However, the impact of the channel drift relative to the simple model employed in this version may be difficult to separate from geophysical change and therefore caution is recommended in evaluating trends derived from this data set.

5. References

Anderson, S. M. and K. Mauersberger, Laser measurements of ozone absorption cross sections in the Chappuis band, *Geophys. Res. Lett.*, 19, 933-936, 1992.

Anderson, S. M., P. Hupalo, and K. Mauersberger, Ozone absorption cross section measurements in the Wulf bands, *Geophys. Res. Lett.*, 20, 1579-582, 1993.

Chiou, E. W., M. P. McCormick, L. R. McMaster, W. P. Chu, J.C. Larsen, D. Rind, and S. Oltmans, Intercomparison of stratospheric water vapor observed by satellite experiments: SAGE II versus LIMS and ATMOS, *J. Geophys. Res.*, 98, 4875, 1993.

Chiou, E.-W., L. W. Thomason, S. P. Burton, H. A. Michelsen, Assessment of the SAGE II version 6.2 water vapor data set through intercomparison with ATMOS/ATLAS-2 Measurements, submitted to JGR, January 2004.

Chu, W. P., E. W. Chiou, J. C. Larsen, L. W. Thomason, D. Rind, J. J. Buglia, S. Oltmans, M. P. McCormick, and L. R. McMaster, Algorithms and sensitivity analyses for SAGE II water vapor retrieval, *J. Geophys. Res.*, 98, 4857, 1993.

Cunnold, D. M., H. J. Wang, L. W. Thomason, J. M. Zawodny, J. A. Logan, and I. A. Megretskaya, SAGE (v.5.96) Ozone Trends in the Lower Stratosphere, *J. Geophys. Res.*, 105, 4445-4457, 2000.

Hervig, M. and M. McHugh, Cirrus Detection using HALOE Measurements, *Geophys. Res. Lett.*, 26, 719-722, 1999.

McCormick, M. P., E.-W. Chiou, L. R. McMaster, W. P. Chu, J. C. Larsen, D. Rind, and S. Oltman, Annual variations of water vapor in the stratosphere and upper troposphere observed by the Stratospheric Aerosol and Gas Experiment II, *J. Geophys. Res.*, 98, 4867-4874, 1993.

Mote, P. W., K. H. Rosenlof, M. E. McIntyre, E. S. Carr, J. C. Gille, J. R. Holton, J. S. Kinnerson, H. C. Pumphrey, J. M. Russell, J. W. Waters, An atmospheric tape recorder: The imprint of tropical tropopause temperatures on stratospheric water vapor, *J. Geophys. Res.*, 101, 3989-4006, 1996.

Newchurch, M. J., E.-S. Yang, D. M. Cunnold, G. C. Reinsel, J. M. Zawodny, and J. M. Russell III, Evidence for slowdown in stratospheric ozone loss: First stage of ozone recovery, *J. Geophys. Res.*, 108(D6), 4507, doi: 10.1029/2003JD003471, 2003.

Rosenlof, K. H., S. J. Oltmans, D. Kley, J. M. Russell, E.-W. Chiou, W. P. Chu, D. G. Johnson, K. K. Kelly, H. A. Michelsen, G. E. Nedoluha, E. E. Remsberg, G. C. Toon, and M. P. McCormick, Stratospheric water vapor increases over the past half-century, *Geophys. Res. Lett.*, 28, 1195-1198, 2001.

SAGE III Algorithm Theoretical Basis Document: Solar and Lunar Algorithm, LaRC 475-00-108, Version 2.1, 26 March 2002.

Shettle, E.P. and S. Anderson, "New visible and near IR ozone absorption cross-sections for MODTRAN", in "Proceedings of the 17th Annual Review Conference on Atmospheric Transmission Models, 8-9 June 1994, G.P. Anderson, R.H. Picard, and J.H. Chetwynd (eds), PL-TR-95-2060, Phillips Laboratory, Hanscom AFB, MA, 24 May 1995, pp. 335-345.

Solomon, S., R. W. Portman, R. R. Garcia, L. W. Thomason, L. R. Poole, and M. P. McCormick, The role of aerosol variability in anthropogenic ozone depletion at northern mid-latitudes, *J. Geophys. Res.*, 101, 6713-6727, 1996.

SPARC/IOC/GAW Assessment of Trends in the Vertical Distribution of Ozone, N. Harris, R. Hudson, and C. Phillips, eds., SPARC Report No.1, WMO-Ozone research and Monitoring Project Report No. 43, 1998.

SPARC Assessment of Upper Tropospheric and Stratospheric Water Vapor, D. Kley, J. M. Russell III, and C. Phillips, eds., WCRP 113, WMO/TD – No. 1043, SPARC Report No. 2, 2000.

Steele, H. M. and R. P. Turco, Separation of aerosol and gas components in the Halogen Occultation Experiment and the Stratospheric Aerosol and Gas Experiment (SAGE) II extinction measurements: Implications for SAGE II ozone concentrations and trends, *J. Geophys. Res.*, 102, 19665-19681, 1997.

Taha, G., L. W. Thomason, and S. P. Burton, Comparison of SAGE II Version 6.2 water vapor with multiple space-based and ground-based instruments, submitted to *JGR*, January 2004.

Thomason, L. W., A diagnostic stratospheric aerosol size distribution inferred from SAGE II

measurements, *J. Geophys. Res.*, 96, 22501-22508, 1991.

Thomason, L. W., G. S. Kent, C. R. Trepte, and L. R. Poole, A comparison of the stratospheric aerosol background periods of 1979 and 1989-1991, *J. Geophys. Res.* 102. 3611-3616, 1997.

Thomason, L. W., L. R. Poole, and T. R. Deshler, A global climatology of stratospheric aerosol surface area density as deduced from SAGE II: 1984-1994, *J. Geophys. Res.*, 102, 8967-8976, 1997.

H. J. Wang, D. M. Cunnold, L. W. Thomason, J. M. Zawodny, and G. E. Bodeker, Assessment of SAGE version 6.1 ozone data quality, *J. Geophys. Res.*, 107 (D23), 4691, doi:10.1029, 2002JD002418, 2002.

Acknowledgments: The authors would like to thank Er-Woon Chiou, Science Applications International Corporation and Ghassan Taha, University of Arizona, for their help in evaluating the intermediate and final versions of this data product. Sharon Burton and Nina Iyer were supported under NASA contract NAS1-02058. John Anderson was supported under NASA Grant NAS1-97042(7).

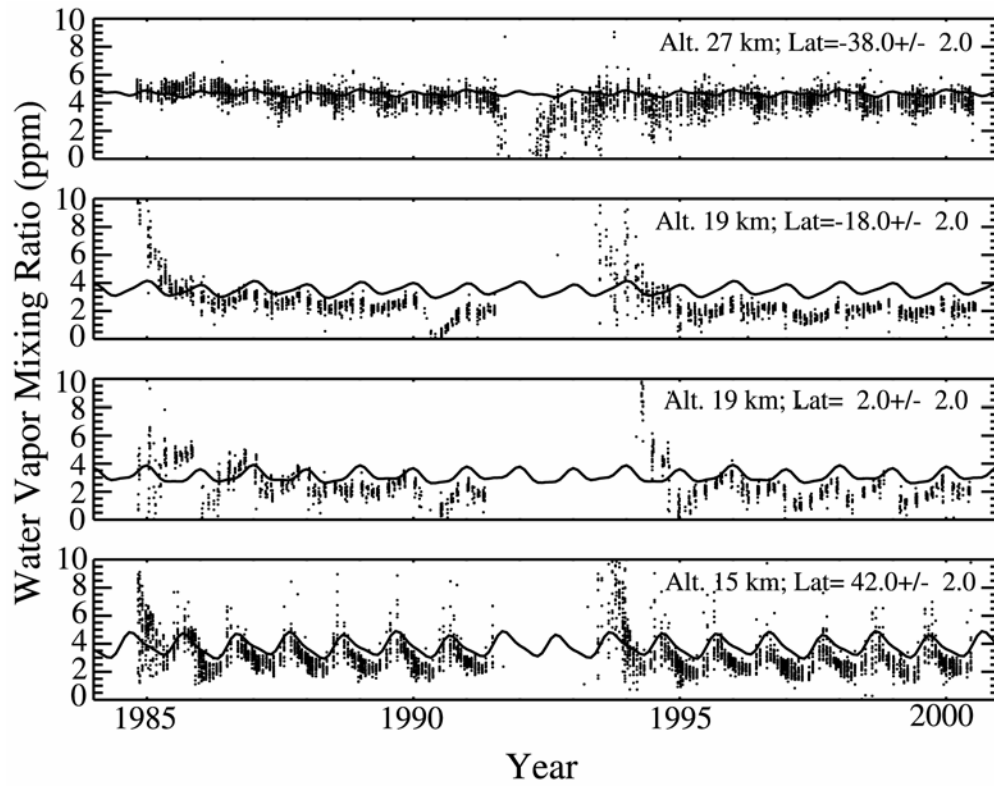


Figure 1. SAGE II version 6.1 water vapor is shown for a variety of altitudes and latitudes in this figure as a scatter plot with the HALOE climatological record superimposed as a the solid line. These results show the problems. These problems include a significant sensitivity to enhanced aerosol (1984-1986, 1990, 1991-1993) and also a tendency for low altitude data to be consistently lower than the HALOE climatology.

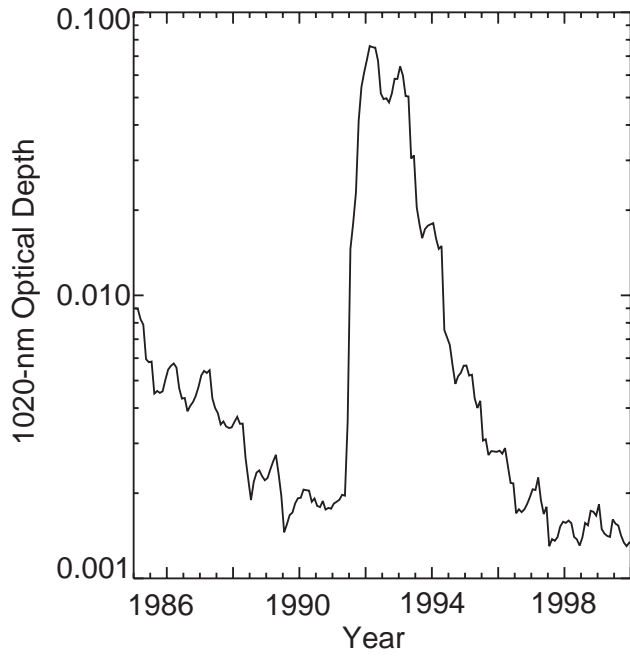


Figure 2. Monthly mean SAGE II 1020-nm optical depth between 30°N and 40°N is shown the period from 1984 through 2000.

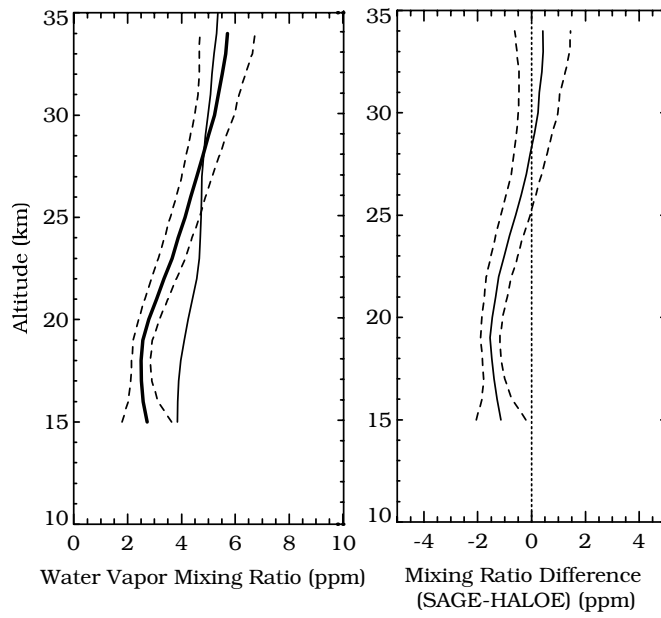


Figure 3. This figure shows the comparison of the 1996-1999 mean Version 6.1 SAGE II water vapor profile (thick line on left with dashed climatological range) with the HALOE climatology.

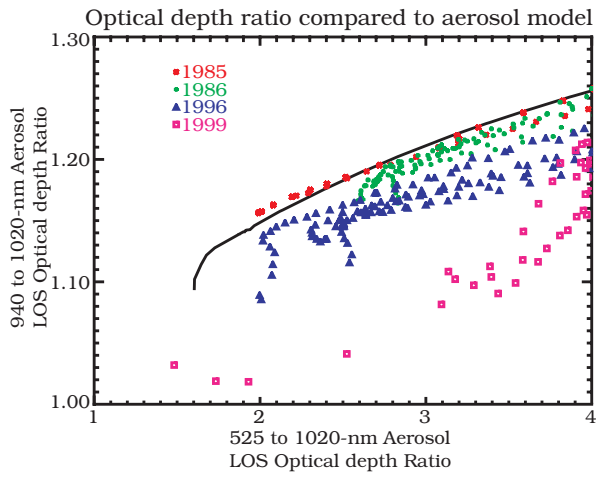


Figure 4. This figure shows a comparison of the 935 to 1020-nm aerosol LOS optical depth versus 525 to 1020-nm aerosol optical depth based on Version 6.2 aerosol model (solid line) with values derived using the HALOE climatology for all January data in 1985, 1986, 1996, 1999.

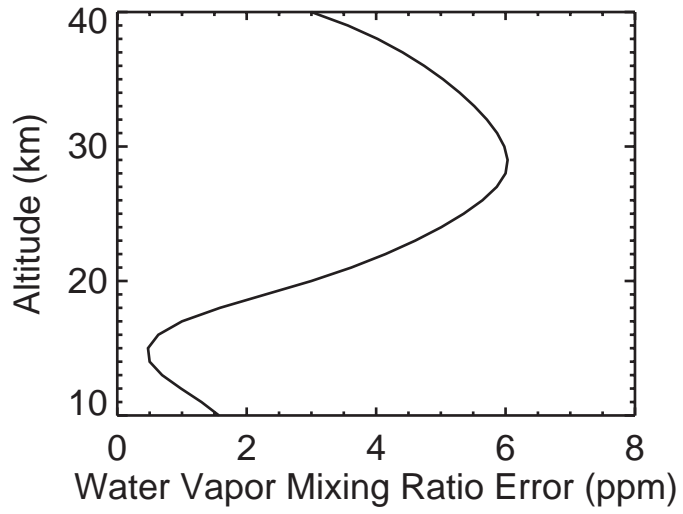


Figure 5. This figure shows the change water vapor mixing ratio for a change in the ozone cross section of 100%.

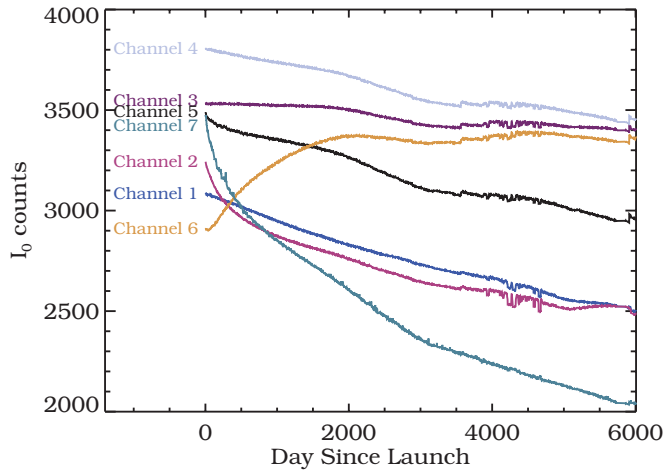


Figure 6. This figure depicts the extraterrestrial count levels for the seven SAGE II channels as a function of days since launch. The channel numbers are in reverse wavelength order or, from channel 1 to 7, 1020, 935, 600, 525, 452, and 386 nm.

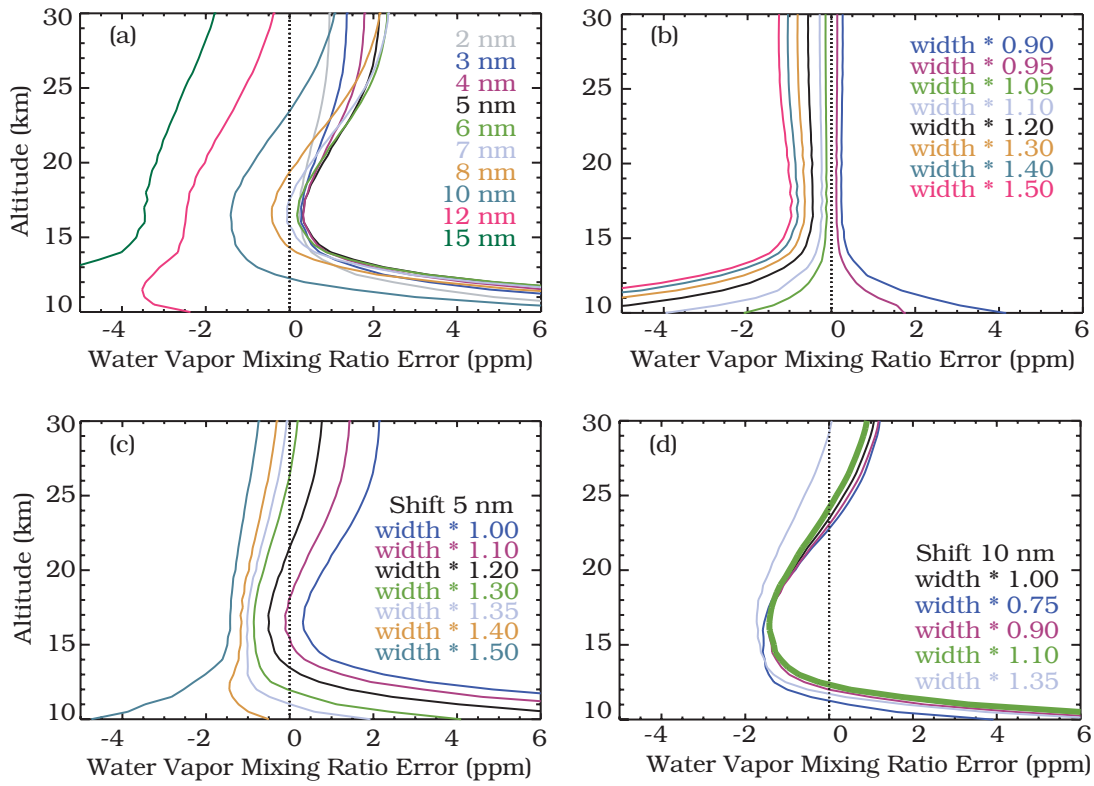


Figure 7. This figure depicts sensitivity of the retrieved water vapor to changes in the spectral response of the water vapor channel. Results are shown for shifts in channel center wavelength (a), change in channel width (b), change in channel width with an increase in location of 5 nm (c), and change in channel width with a shift in location of 10 nm (d). The final position (10 nm, +10%) is shown as a thick line in frame (d).

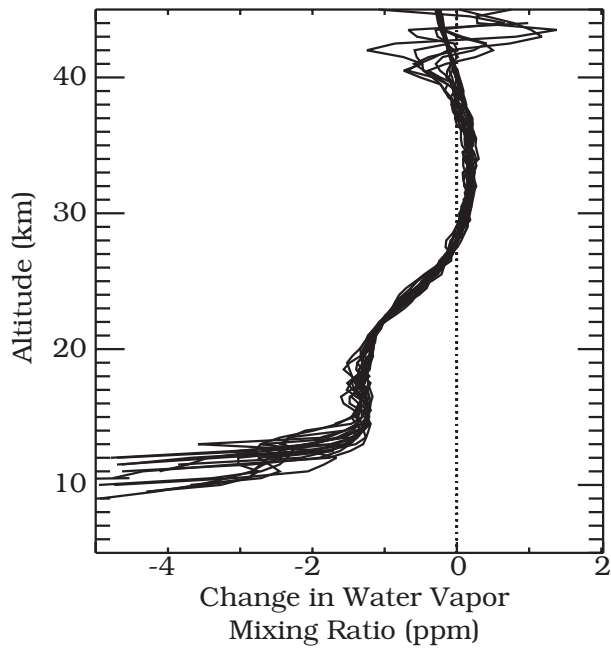


Figure 8. Impact of the proposed 10 nm shift and 10% increase in channel width on 18 water vapor profiles from June 2002 are shown in this figure. The results (Version 6.1-Version 6.2) demonstrate that the impact on actual measurements of the proposed shift mimic the experimental results.

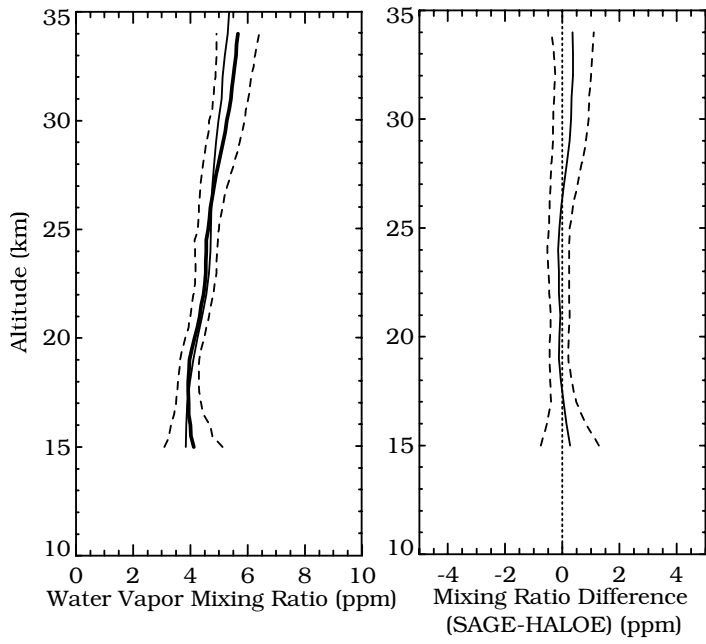


Figure 9. This figure is the Version 6.2 equivalent of Figure 3 showing SAGE II water vapor (thick line on left) departures from HC, in this case, after the moving the channel location to 945 nm with a FWHM of 33 nm.

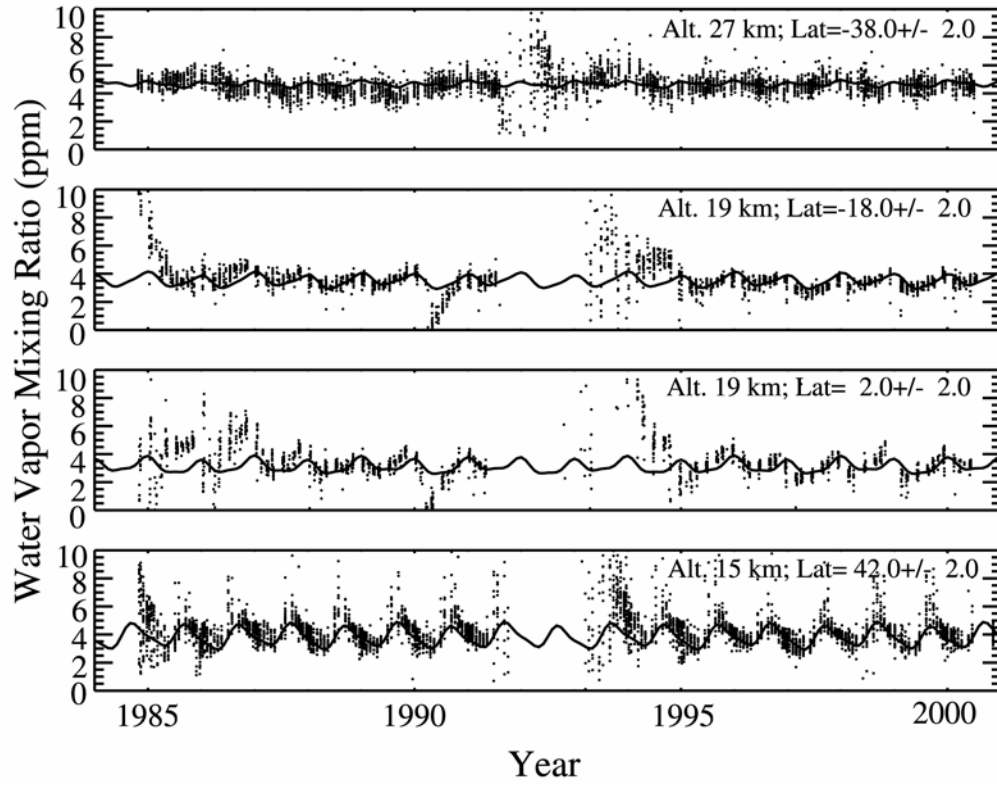


Figure 10. SAGE II version 6.2 water vapor is shown for a variety of altitudes and latitudes in this figure as a scatter plot with the HALOE climatological record superimposed as the solid line.

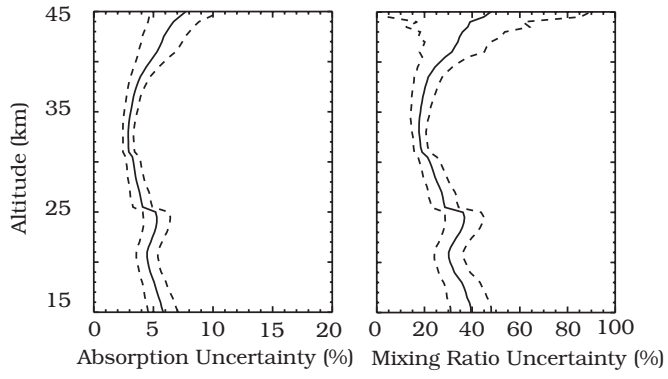


Figure 11. Mean absorption uncertainty and the resulting water vapor mixing ratio uncertainty is shown in this figure for northern mid-latitudes in June 2002.

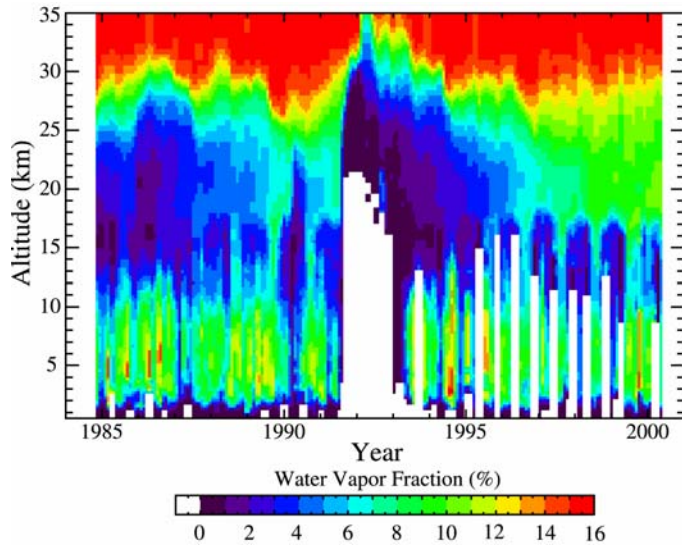


Figure 12. This figure depicts the fraction of the signal in the SAGE II water vapor channel from water vapor for 10°S to 10°N between 1985 and 2001. The other components in this channel include scattering by molecules and aerosol and ozone absorption.

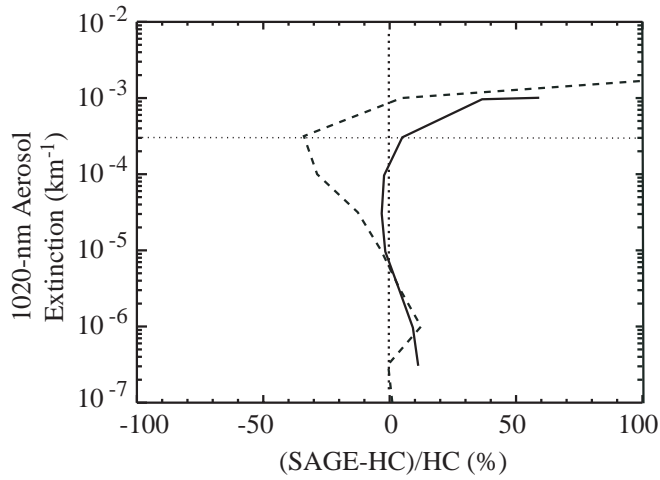


Figure 13. This figure depicts the difference between SAGE II water vapor and the HALOE water vapor climatology for the period 1996 to 1999 for Version 6.1 (dashed) and Version 6.2 (solid). The horizontal line at $3 \cdot 10^{-4} \text{ km}^{-1}$ marks the +5% departure for Version 6.2; the comparable value for Version 6.1 is $\sim 2 \cdot 10^{-5} \text{ km}^{-1}$ (-5%).

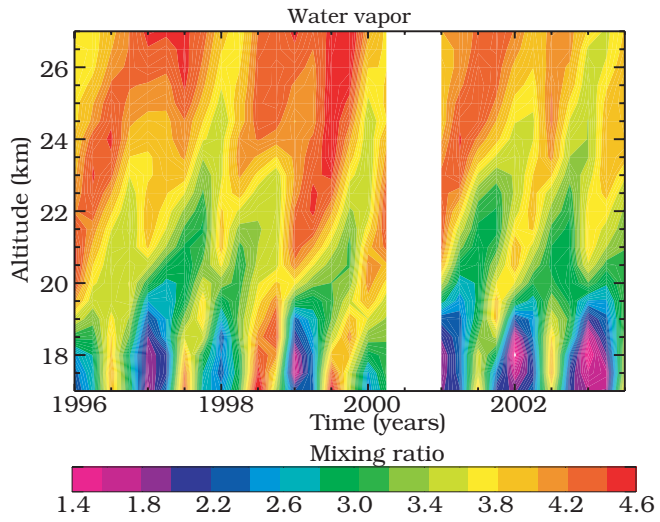


Figure 14. This figure depicts the water vapor mixing ratio between 10°S and 10°N between 1996 and 2003 and clearly shows the well-known tape-recorder effect.